Heiskari, Janne; Romanoff, Jani; Laakso, Aleksi; Ringsberg, Jonas W.

On the thickness determination of rectangular glass panes in insulating glass units considering the load sharing and geometrically nonlinear bending

Published in:
Thin-Walled Structures

DOI:
10.1016/j.tws.2021.108774

Published: 01/02/2022

Document Version
Publisher's PDF, also known as Version of record

Thin-Walled Structures 171 (2022) 108774

Contents lists available at ScienceDirect

Thin-Walled Structures

journal homepage: www.elsevier.com/locate/tws

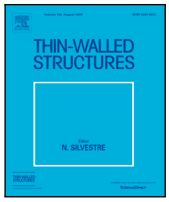

Full length article

On the thickness determination of rectangular glass panes in insulating glass units considering the load sharing and geometrically nonlinear bending

Janne Heiskari [a,*], Jani Romanoff [a], Aleksi Laakso [b], Jonas W. Ringsberg [c]

[a] Department of Mechanical Engineering, Aalto University School of Engineering, Espoo, Finland
[b] Meyer Turku Oy, Turku, Finland
[c] Department of Mechanics and Maritime Sciences, Chalmers University of Technology, Gothenburg, Sweden

ARTICLE INFO

Keywords:
Insulating glass unit
Lightweight ship structures
Load sharing
Nonlinear Finite Element Method
Plate theory
Ship classification

ABSTRACT

The number and size of windows has increased in large cruise ships, especially on the top decks. They have therefore become a weight and stability-critical component of the structure. Their thickness is determined according to the classification rules which are generalized for all type of passenger ships. That is, the provided formulae are based on linear-elastic, small deformation, plate theory and therefore more suitable for smaller windows in non-weight critical applications. However, majority of the windows are large insulating glass units (IGUs) that exhibit two effects that the rules do not currently consider: development of membrane stresses in the glass panes at large deflections due to the von Kármán strains (geometric nonlinearity) and interaction of the glass panes due to the internal cavity pressure between them (load sharing). Both increase the load bearing capacity of the IGUs. Therefore, extension to the thickness determination is needed for achieving the lightweight design. This paper uses nonlinear Finite Element Method to study the IGUs static response under uniformly distributed load considering the effects. The response consists of principal stress and deflection of the panes, and the cavity pressure. Validation is carried out by experimental results from scientific literature. Case study on typical panes from cruise ships indicate that considering the two beneficial effects, the thickness of the glass panes in the IGUs may potentially be reduced between 26–54 % with respect to the classification rule-based design. That is, by using the same allowable principal stress criterion between the linear and nonlinear predictions.

1. Introduction

The size of modern cruise ships has increased in the recent years to accommodate more passengers and amenities. Consequently, the ship's structural weight has increased that negatively affects its operational efficiency, stability and building cost, to name a few. Using lightweight structures and materials instead of conventional steel structures helps to save weight [1–9]. While the steel structures lighten due to the improved design and manufacturing methods, glass is used in increasing proportions to enable better immersion for the passengers. Not only the number and size of individual windows has increased, but also large glass structures are built with an area of several hundred square meters. The corresponding weight contribution and stability impact can be considerable as majority of these large windows are located on the top decks (Fig. 1).

As the area of the windows increases, their thickness should be reduced to achieve the lightweight design without harming the safety. The way to do this is to increase the strength of the glass or make the stress assessment more accurate. Since only strengthened glasses (thermally toughened or chemically strengthened[1]) are allowed for in the considered applications,[2] this paper focus on the latter, i.e. on the weight-savings based on more advanced response calculation of the windows.

These windows are insulating glass units (IGUs) that consist of at least two glass panes separated by a hermetically sealed cavity (Fig. 1). The cavity is often filled with Argon gas for better thermal insulation. A structurally beneficial interaction occurs between the glass panes due to the gas pressure changes in the sealed cavity, known as load sharing. Furthermore, it is well-known that at large deflections the von Kármán strains increase the stiffness of the panes and also reduce the bending-induced stresses due to the activated membrane-mechanism.

However, the design of the IGUs in ships is done according to the rules and regulations by the classification societies (e.g. [11–13])

* Corresponding author.
E-mail address: Janne.Heiskari@aalto.fi (J. Heiskari).

[1] Chemically strengthened glass is allowed only by some classification societies given that it is in laminated construction and its strength has been demonstrated to be at least equivalent to that of thermally toughened glass.

[2] According to the classification rules for passenger ships.

https://doi.org/10.1016/j.tws.2021.108774
Received 26 April 2021; Received in revised form 15 September 2021; Accepted 2 December 2021
Available online xxxx

Nomenclature

A	area of the glass pane [mm^2]
D	flexural stiffness [Nmm]
E	Young's modulus [MPa]
H	design pressure head [m]
M	bending moment [Nmm]
N	number of moles of gas [mol]
R	ideal gas constant [J K^{-1} mol^{-1}]
Re	relative error [%]
T	temperature of the gas in the cavity [K]
V	volume of the cavity [mm^3]
a	longer side length of a rectangular glass pane [mm]
b	shorter side length of a rectangular glass pane [mm]
m	positive integer [–]
n	positive integer [–]
p	pressure of the gas in the cavity, in Equations [MPa], otherwise [kPa]
$\overline{p}$	uniformly distributed load, in Equations [MPa], otherwise [kPa]
q	design load [kN/m^2]
s	spacer thickness [mm]
t	glass pane thickness [mm]
u	deformation in x-direction [mm]
v	deformation in y-direction [mm]
w	deformation in z-direction (deflection) [mm]
x, y, z	coordinate
Δt	time increment for the current substep [s]
β	aspect ratio factor [–]
ϵ	strain [–]
ν	Poisson's ratio [–]
ρ	density [kg/m^3]
σ	stress [MPa]
φ	mean value of shape function for rectangular pane [–]
$\dot{(\,)}$	incremental change of the enclosed quantity

Subscripts

+	maximum principal
0	reference value at the time of sealing
1	glass pane 1
2	glass pane 2
a	allowable design flexural
b	bending
i	glass pane number
$m, \upsilon K$	membrane von Kármán
n	end of previous substep
r	required minimum
t	total
x, y, z	coordinate

or by nationally or internationally recognized equivalent standards (e.g. ISO 11336-1 [14]), where the main assumptions are that the cavity pressure does not exist and linear-elastic Kirchhoff plate theory is valid. The resulting minimum required thickness for a monolithic glass pane is determined depending on its size, shape, and location. Table 1 reviews the rules and Fig. 2 the outcomes. The data referred to in Fig. 2 (right-hand side) has been derived by the linear plate theory (Eqs. (A.1)–(A.3)) and by computing the maximum principal stress equal to 40 MPa. It is clear from Fig. 2 that the rules are based on this theory.

The linear theory is considered accurate at small deflections ($w < t$). However, this assumption does not hold when ships operate in extreme conditions and encounter high pressure levels. For instance, ship windows tested for ultimate loads up to 170 kPa exhibited geometric nonlinearity approximately when the center-of-pane deflection equaled the thickness of the pane ($w \approx t$) [15]. The stress increase becomes degressive for larger deflection ($w > t$) which linear calculation cannot capture. Hence, the overestimation of the stresses results in underestimation of the load bearing capacity of the panes. Similar underestimation takes place when neglecting the load sharing effect.

Some amount of the load applied externally to one pane of the IGU is transferred to the adjacent pane via the enclosed gas. When the directly loaded pane deflects, the cavity volume decreases and consequently the internal pressure increases, which acts on the indirectly loaded pane. McMahon et al. [16] studied the nonlinear load sharing experimentally and demonstrated its significance. For instance, a unit with two equally thick glass panes shared an uniform pressure load almost equally between the panes (49 % and 51 %). Vallabhan and Chou [17] studied the load sharing using nonlinear plate theory in an iterative procedure. They showed how the maximum deflections and principal stresses of the panes evolve due to the von Kármán effect coupling the membrane stresses to the bending stresses by using the Finite Difference Method and non-dimensional design charts. They also found that the maximums stress moves toward the corners of the plate for increasing pressures. Wörner et al. [18] conducted a similar study but they used a simple approximation and Finite Element Method to solve the maximum deflection of the panes, including the nonlinearities, which was then used to determine the load sharing. Galuppi and Royer-Carfagni [19] proposed "Betti's analytical method" (BAM) for calculating the load sharing in IGUs with two glass panes. It is an approximation model based on linear-elastic plate theory to compute the volumetric change of the cavity in IGUs. They showed that load sharing is most beneficial for thin and large glass panes, like ships have. The method was extended for IGUs with multiple panes in [20]. In practical design, the load sharing is often considered through standards, e.g. EN-16612 [21] in building architecture. While these studies report results with satisfactory accuracy, they lack the design freedom in terms of boundary conditions and glass shapes. Extension of the methods towards ship design are needed.

Therefore, this paper uses a FE technique where the interaction of the glass panes and the gas is embedded in the model. The influence of the large deflections on the gas pressure is therefore automatically considered. Furthermore, the FEM is applicable to any IGU construction under various loads, boundary conditions and assumptions. Hence, this is a convenient approach to study the influence of the geometrically nonlinear bending and the load sharing on the deflections and the stresses of the glass panes in the IGUs. The model is validated by BAM [19] and MEPLA ISO [22] on linear basis. On nonlinear basis, experimental results from [16] are used to validate the model.

Using the validated model, the goal is to provide a better understanding for designing these weight critical glasses in ships by reflecting the obtained knowledge of the reduced stress state on the prescribed thickness determination rules presented in Table 1.

2. Large deflection of panes

The equations for the glass pane thickness determination discussed in Section 1 and presented in Appendix (Eqs. (A.1)–(A.3)) are suitable for Kirchhoff plates subjected to small deflections, where it is reasonable to assume that the mid surface of the plate does not strain during bending. Then, the corresponding load carrying mechanism consist

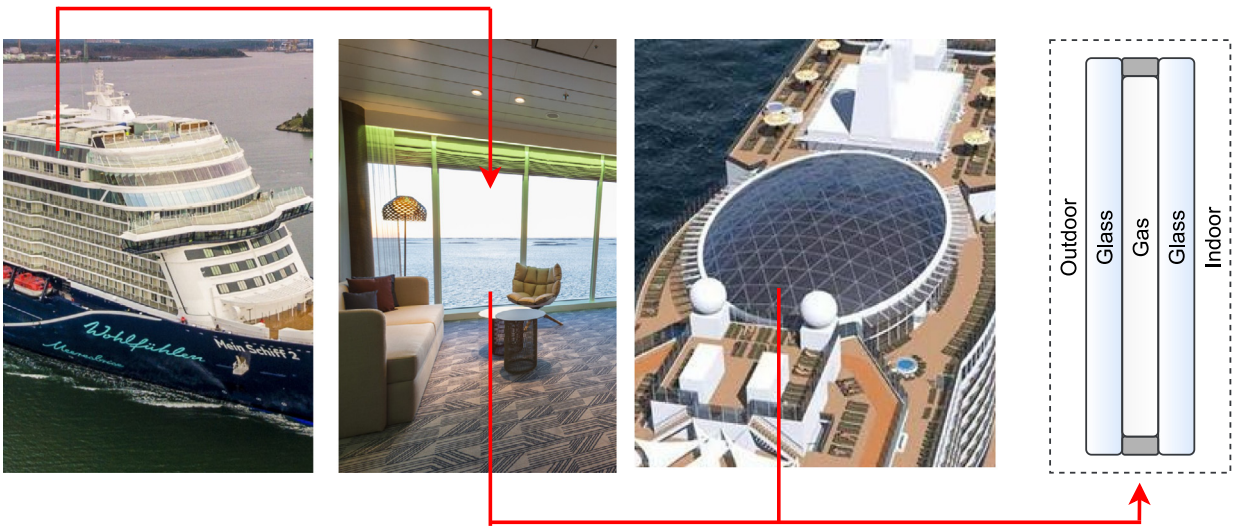

Fig. 1. Examples of windows onboard the cruise ships: two first from the left-hand side are from Mein Schiff 2, courtesy of Meyer Turku Oy; third is SkyDome of M/S Iona, courtesy of Francis Design [10]; the last one is a cross-section sketch of an insulating glass unit.

Table 1
Thickness determination of monolithic rectangular glass panes in ships according to different design rules.

	Lloyd's Register [11]	DNV GL [12]	ISO 11336-1 [14]
Thickness	$t_r = b\sqrt{\frac{H\beta}{4000}}$	$t_r = \frac{b}{200}\sqrt{q\beta}$	$t_r = b\sqrt{\frac{q\beta}{1000\sigma_a}}$
β	$\begin{cases} 0.54(a/b) - 0.078(a/b)^2 - 0.17 & \text{for } a/b \le 3 \\ 0.75 & \text{for } a/b > 3 \end{cases}$	Fig. 2	Fig. 2

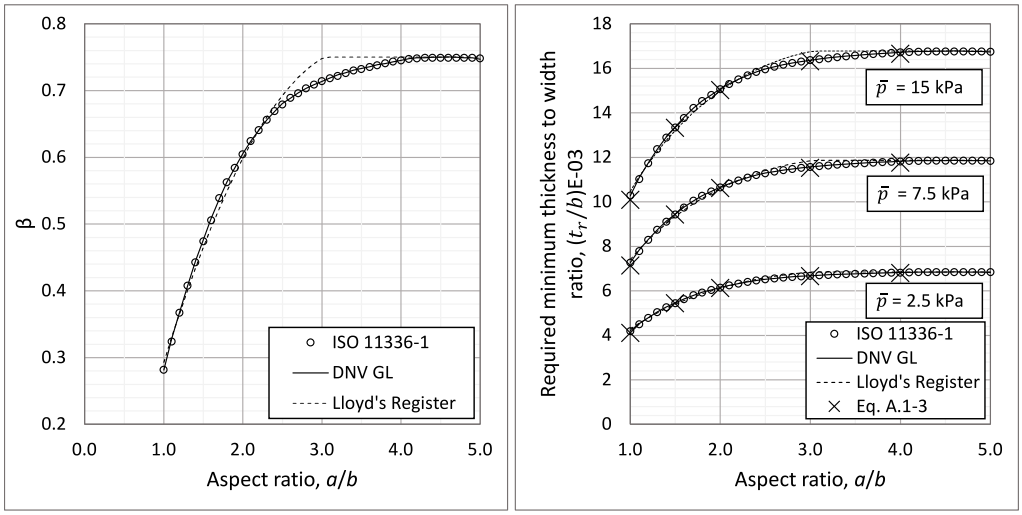

Fig. 2. On the left-hand-side are the beta factors. On the right-hand-side are the resulting required minimum thickness to width ratios for multiple aspect ratios by using the equations from Table 1 and Eqs. (A.1)–(A.3) with 40 MPa design flexural stress.

of only the bending action. However, when the deflection increases and reaches some ratio, $\frac{w}{t}$, the mid surface starts to stretch and the load carrying mechanism is accompanied by the resulting membrane forces (right-hand side in Fig. 3). That is, the in-plane stretching of the mid surface resists the out-of-plane load. In the case of glass panes, the increased strength from the glass post-processing (tempering or chemical strengthening) allows for the geometric nonlinearity to be very significant. This increases the load bearing capacity of the glass panes, as shown in Fig. 3 (left-hand side).

Mathematically, this is considered by adding the von Kármán terms (highlighted) in the set of strain equations for the Kirchhoff plates [24]:

$$\begin{aligned} \varepsilon_{xx} &= \frac{\partial u}{\partial x} + \frac{1}{2}\left(\frac{\partial w}{\partial x}\right)^2 - z\frac{\partial^2 w}{\partial x^2} \\ \varepsilon_{yy} &= \frac{\partial v}{\partial y} + \frac{1}{2}\left(\frac{\partial w}{\partial y}\right)^2 - z\frac{\partial^2 w}{\partial y^2} \\ \varepsilon_{xy} &= \frac{1}{2}\left(\frac{\partial u}{\partial y} + \frac{\partial v}{\partial x} + \frac{\partial w}{\partial x}\frac{\partial w}{\partial y} - 2z\frac{\partial^2 w}{\partial x \partial y}\right). \end{aligned} \tag{1}$$

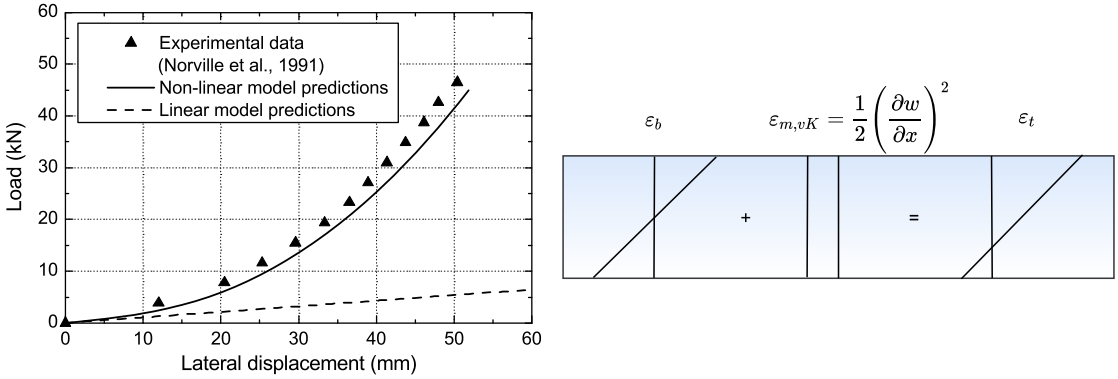

Fig. 3. On the left-hand side is comparison of nonlinear and linear predictions with experimental results for thermally toughened glass pane (1676.4 × 1676.4 × 5.66 mm) [23]. On the right-hand side is the role of von Kármán strains on the overall stress state through the thickness (bending + membrane = total).

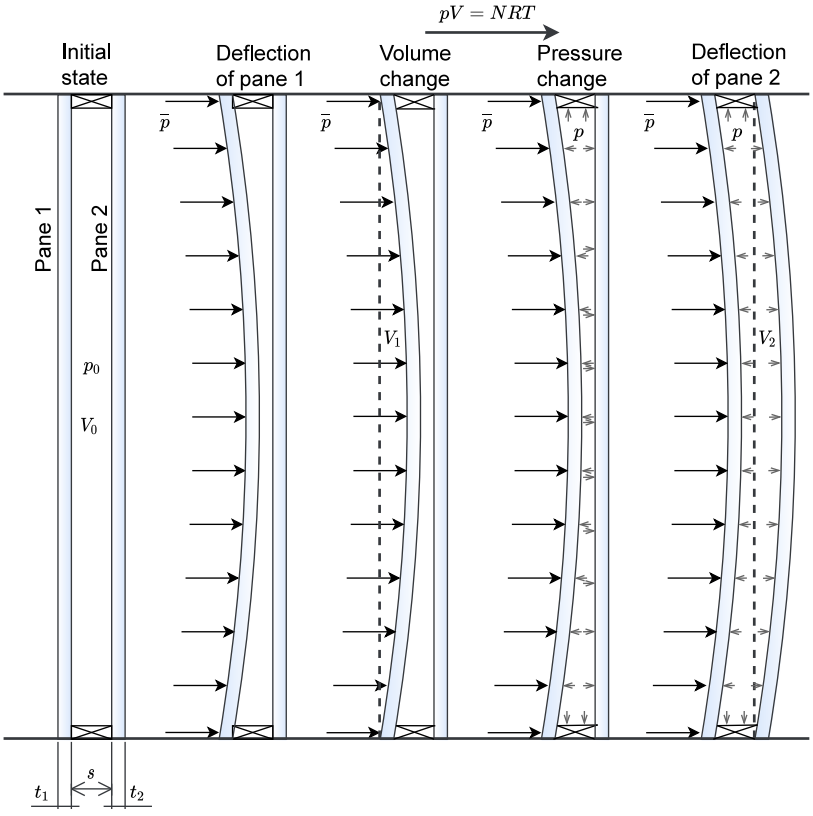

Fig. 4. Free body diagram of an IGU under external load including the load sharing.

The squared terms couple the in-plane and out-of-plane displacements, i.e. the bending and membrane actions at large deflections. These become dominant after the deflection grows larger than the thickness. Therefore, neglecting the geometric nonlinearity heavily underestimates the deflection of thin and large glass panes.

3. Load sharing

The insulating glass unit consist of the glass panes, the spacers, and the cavity. The cavity is hermetically sealed for its purpose to provide thermal insulation. This also allows for the load sharing to occur. If the cavity leaks, the insulation properties weaken and it absorbs moisture which accumulates on the glass panes, even if the spacers are filled with moisture absorbing desiccant. Since the IGUs are visible to the passengers at all times, the fogging impairment gives a clear indication for a repair. For this reason, we argue that it does not pose any additional risks when including the load sharing effect in the design process.

The load sharing is governed by the ideal gas law, $pV = NRT$. The cavity has some initial pressure depending on the conditions at time of sealing. For this paper, we assume that there is no initial deflection of the panes due to temperature change, atmospheric pressure change or altitude change (climate loads [25]), i.e. the IGU is at equilibrium and hence, the initial cavity volume is the pane area times the spacer thickness. An external load is applied on the outer pane. Once the directly loaded pane deflects, the cavity volume variation changes the internal pressure, which causes the indirectly loaded pane to deflect, see Fig. 4. Because the volume has changed again, a new pressure is calculated, and so on, until the system is at equilibrium (Fig. 5). For solving this iterative process, the ideal gas law is extended to solve incremental volume change at certain time-steps

$$\dot{V} = \frac{1}{\Delta t}\left(V - V\frac{p_t}{p_{n,t}}\frac{T_{n,t}}{T_t}\right) = -\frac{V}{p_{n,t}}\dot{p} + \frac{V_n}{T_{n,t}}\dot{T}. \tag{2}$$

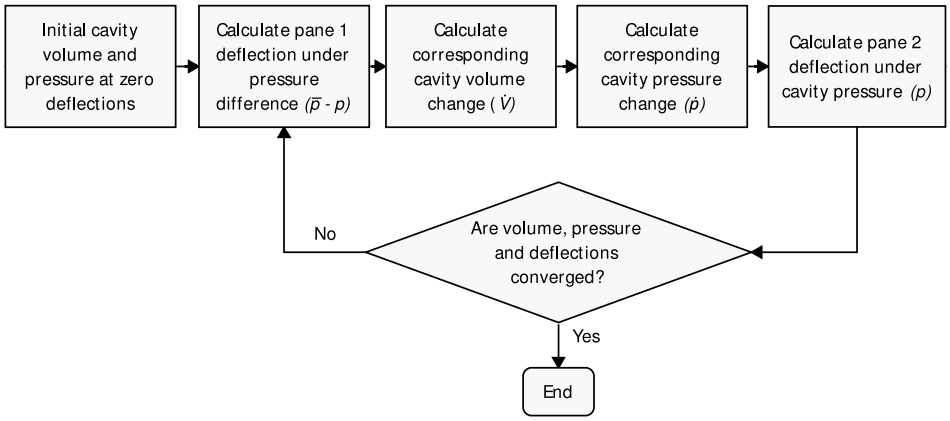

Fig. 5. Iterative process for solving the equilibrium state with gas filled cavity.

where the subscripts "n" and "t" denote the value at the end of the previous substep and the total value, respectively. The total pressure and temperature consist of the current value and the reference value ($p + p_0$ and $T + T_0$). Newton–Raphson method is used [26] for this nonlinear analysis. The formulation of these coupled system of the solids and the gas is described in [27].

On linear basis, the Betti's analytical method can be used to determine the pressure increase due to the actions on the pane [19,28]. Consider an IGU with two glass panes that have thicknesses "t_1" and "t_2", respectively. The panes are separated by a spacer with thickness "s". The panes are rectangular with longer and shorter sides, denoted with "a" and "b", respectively. An uniform external pressure, $\overline{p}$, is applied on the surface of pane 1. The generated cavity pressure variation, p, is calculated with the following formula:

$$p = \frac{\frac{1}{D_1}\varphi}{\left(\frac{1}{D_1} + \frac{1}{D_2}\right)\varphi + \frac{V_0}{A^3 p_0}}\overline{p}, \tag{3}$$

where:

$D_i = \frac{Et_i^3}{12(1-\nu^2)}$ is the flexural stiffness of the ith pane (1,2) [Nmm].

φ is the mean value of the shape function on the plate area [–].

The mean value of the shape function for rectangular pane with sides "a" and "b" is:

$$\varphi = \frac{64a^2}{\pi^8 b^2}\sum_{m=1}^{\infty}\sum_{n=1}^{\infty}\frac{1}{m^6 n^2\left(1 + \frac{n^2a^2}{m^2b^2}\right)^2}. \tag{4}$$

One may use the cavity pressure obtained from Eq. (3) in Eqs. (A.1)–(A.4) to calculate the IGU response on linear basis. To correctly include the load sharing, the uniformly distributed load is replaced with $\overline{p} - p$ and p for pane 1 and pane 2, respectively. Alternatively, the linear response can be solved using MEPLA ISO[3] [22].

4. Finite element analysis of insulating glass units

Finite Element Method-based approach is exploited to model simultaneously the nonlinear pane response accounting the von Kármán strains and the iterative internal pressure increase in the cavity. ANSYS® Mechanical™ is used. Alternatively, one may use e.g., ABAQUS [29] or RFEM with RF-GLASS Add-on module [30]. However, shell elements are preferred (Section 4.2), while the latter uses solid elements. The ANSYS model consist of two monolithic glass panes, gas filled cavity, and four spacers. The spacers merely create the volume of the cavity with the glass panes, but for simplification, they are not structurally considered in the analysis, i.e. they are modeled with low stiffness, small thickness, and all nodes bound. In reality, the spacers stiffen the IGU in bending to some degree [31]. Therefore, omitting their influence on the response is a conservative approach as the FE analyses will predict slightly larger deflections. Besides, the spacers are part of detail design phase and experimental work is required for finding their true stiffness in the respective case.

4.1. Boundary conditions and loads

Two boundary conditions (BCs) are used: (1) BC_{ss}, the edges are simply supported, i.e. all translations of the edges are fixed while rotations are free; (2) BC_{free}, in-plane translations of the edges are free while lateral translation is fixed, and rotations are free. In the latter condition, the middle nodes of both panes are restrained in the in-plane direction and their rotation around z-axis is fixed for the sake of having fully constrained model (Fig. 6). This boundary condition also mimics the setup used in the experiments by McMahon et al. [16], see Fig. 7. The aluminum brackets pressing the neoprene gaskets against the glass are loosely tightened to minimize the in-plane and rotational restraints of the IGU. In the current study, both conditions are used in nonlinear analysis to study the impact of the BCs on the development of the von Kármán strains at large deflections. In this way the response is studied at two theoretical limits, while the real conditions in ships lay somewhere in between. Uniformly distributed load is applied on the surface of pane 1, referred to as the directly loaded pane. This load represents a short duration load, such as wind. This is a simplified approach, as real glass structures are subjected to different combination of loads with varying duration that alter the IGUs response and its lifetime [32]. For instance, the climate loads are omitted, though they can be included as body loads and initial conditions with good accuracy [33] for future studies.

4.2. Glass elements

This model will be used in future studies where the thickness of the panes is optimized while the element sizes should remain constant. Therefore, it is convenient to choose an element for the glass panes with nodes only at the mid-plane. We exploit shell elements (Fig. 8) instead of solids for the glass panes as this secures computational accuracy and

[3] MEPLA ISO is a freeware software for calculating the response of insulating glass units consisting of two or three glass panes. The software works on linear basis and uses analytical approach of double Fourier Series to calculate maximum deflections and maximum principal stresses of linearly simply supported IGU on its all 4 edges (influence of spacers excluded). The accuracy is based on Kirchhoff's plate theory and because geometric nonlinearities are neglected, the solution is valid for deflections smaller than half the plate thickness ($w < \frac{t}{2}$). The cavity behavior is governed by the ideal gas law, but the magnitude of the cavity pressure is not presented in the software solution.

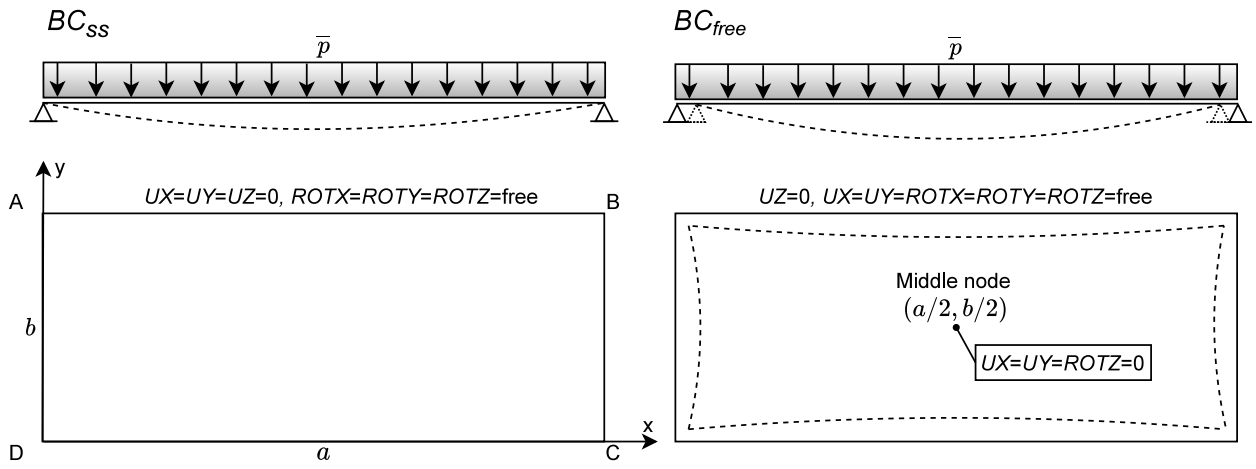

Fig. 6. Illustration of the boundary conditions and the corresponding deformed shapes. The edge conditions are equal for pane 1 and pane 2 (AB1=BC1=CD1=DA1=AB2=BC2=CD2=DA2). Middle node of both panes is restrained from moving in the in-plane directions and rotating around z-axis in BC_{free} to have fully constrained system.

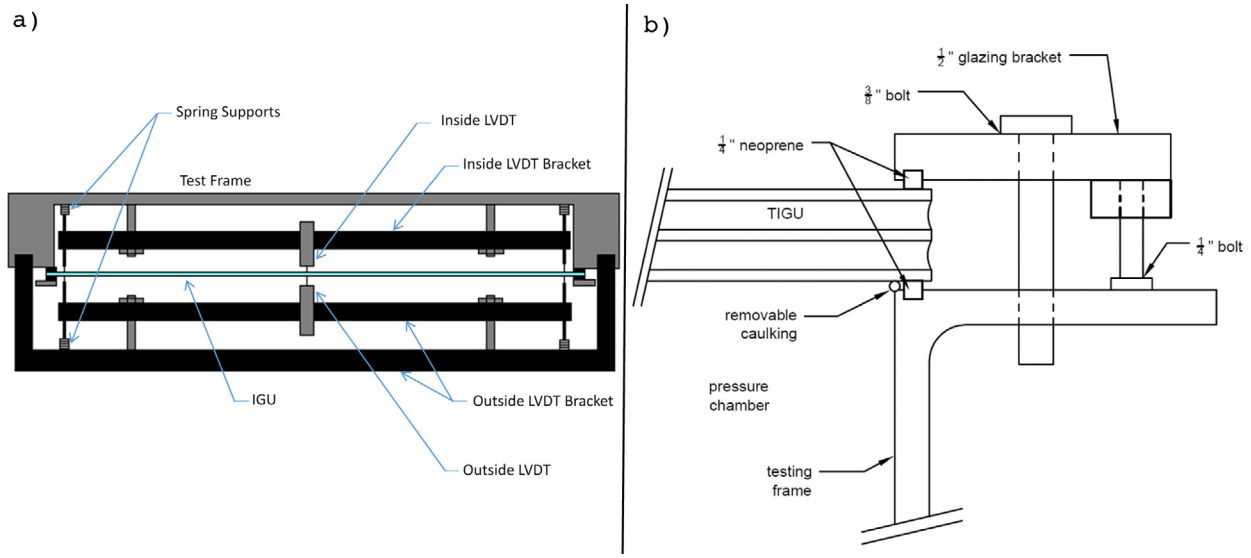

Fig. 7. Experimental setup from [16]: (a) is the bracket for deflection measurement instruments (LVDT) and (b) shows the supporting mechanism of the studied double and triple IGUs (TIGUs are excluded in the current study).

efficiency in applications where the pane thickness is small.[4] This is also to avoid any shear or membrane locking at large deflections that may occur when using solid elements with high aspect ratios. Further, thin shells are a natural choice over the solids since the classification rules are based on them, as shown earlier. SHELL181 elements are used with full integration (KEYOPT(3) = 2), though the difference to reduced integration is in order of 0.1 % in the considered out-of-plane bending of thin-walled plates. The accuracy of the elements is governed by Mindlin–Reissner plate theory, also called as First-order shear deformation theory (FSDT), which includes transverse shear deformation through the thickness [34]. FSDT is suitable for thin and moderately thick panes. When the glass panes are relatively thin ($\frac{thickness}{width} < \frac{1}{10}$), like in this study, they act like Kirchhoff's plates and hence FSDT and Kirchhoff's plate theory are both suitable. Therefore, the FEM and analytical results are comparable on linear basis. However, sometimes triangular, or other odd shaped thick windows are used in ships. Then, the thickness to characteristics length ratio increase may require at least FSDT for accurate prediction of the response.

4.3. Gas elements

The gas is modeled with 3-D hydrostatic fluid elements, HSFLD242, presented in Fig. 8. They are pyramid shaped elements specifically designed to model fluids enclosed by solids. The nodes at the base have translation degree-of-freedoms (DOFs) and are shared with the structural shell elements they are attached to. The base has either 4 or 8 nodes depending on how many nodes the structural element has. The pressure node "Q" at the apex of the pyramid has hydrostatic pressure (HDSP) DOF and is shared with the corresponding nodes of all the hydrostatic fluid elements in the cavity. Hence, the density, pressure and temperature of the gas are presented uniformly through this one node. That is, they are equal for all the HSFLD elements.

[4] We have verified that shell elements (SHELL181) are as accurate as solid-shell elements (SHOLHS190) in this study considering the presented boundary conditions, loading conditions, responses and design criteria (i.e., cases in Fig. 17 and Table 5). The difference between the elements in maximum deflection and maximum principal stress is in order of 0.05 % and 0.1 %, respectively. Solid-shell element gives a better representation of the in-plane deformation of the edges, as it is 3-dimensional, but the maximum absolute difference between the elements is in order of 0.1–0.3 mm, which is insignificant considering the required 10 mm overlap.

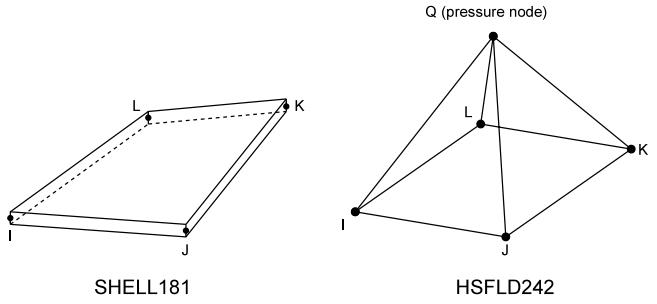

Fig. 8. Structural SHELL181 element [35] and HSFLD242 element [36].

4.4. Model and mesh

The glass and the spacers are meshed with 4-node SHELL181 elements. The pressure node "Q" is placed at the center of the cavity. The HSFLD242 elements are "coated" on the surfaces of the structural elements facing the cavity. Because the hydrostatic fluid elements are attached to the structural shell elements, the number of HSFLD242 and SHELL181 elements are exactly equal (Fig. 9). Further, with high mesh density, the local curvature in the shell element is minor along the element and thus the linear variation of the deflection dominates the response. That is, there is no significant gap between the attached SHELL181 and HSFLD242 elements due to the latter not having rotational degrees of freedom. The coupling is described in ANSYS Theory Ref. [27]. Detailed process of meshing the cavity with the HSFLD242 elements is presented [33].

4.5. Post-processing

The studied response consists of: (1) deflection of both panes; (2) maximum principal stress of both panes; (3) the generated pressure variation in the cavity; (4) in-plane deformation of the edges. The deflection is observed to ensure that the glass panes do not contact each other. This is, however, unlikely as in most cases the gas pressure reaches magnitude of 40–49 % of the external load, i.e. the panes experience similar load, deflection and stress. The classification societies use a limiting value for the maximum principal stress. Similarly, they require a certain overlap between the glass panes and the supporting structure, which is why it is important to record the in-plane movement of the edges. The maximum in-plane deformation of both panes is used for this, as shown in (Fig. 10).

The in-plane movement and the deflection of the indirectly loaded pane is always less due to the compressibility of the gas. Further, because the ideal gas is unable to resist shear deformation, the maximum principal stress is maximum on the tension side of both panes and zero, or close to zero, on the compression side (Fig. 11). The absolute maximum stress may be on either pane, depending on their thickness configuration.

5. Results

In this chapter, the presented FE model is first validated on linear basis using BAM [19] and MEPLA ISO [22]. Then, the model is validated on nonlinear basis using the experimental results by McMahon et al. [16]. The IGU dimensions for validation are presented in Table 2. Both, linear and nonlinear, analyses are used to study the cavity pressure generation. Finally, the validated model is used on nonlinear basis to conduct a case study to determine the required minimum thickness for the monolithic glass panes in an IGU for three different load cases. These results are compared to the design approaches suggested by the classification societies and ISO 11336-1 standard.

Table 2
IGU dimensions for validation of the FE model. The dimensions are same as used in [16].

	IGU A	IGU B
a [mm]	1260	1260
b [mm]	750	750
t_1 [mm]	5.7	5.7
t_2 [mm]	5.7	3.1
s [mm]	13	13

Table 3
Comparison of generated cavity pressure on linear basis.

	IGU A	IGU B
p, BAM [kPa]	0.47083	0.13623
p, ANSYS [kPa]	0.47063	0.13630
Re [%]	0.0425	0.0514

5.1. Linear analysis

Pane 1 is subjected to uniformly distributed load of 1.0 kPa. The generated cavity pressure is recorded from ANSYS and BAM (Eq. (3)). Deflection of both panes are plotted along line $b/2$ every 42 mm from $x = 0$ to $x = a$. In analytical solution, the deflection is calculated with Eq. (A.4) by replacing the uniformly distributed load with $\bar{p} - p$ and p for pane 1 and pane 2, respectively. Based on the results presented in Fig. 12 and Table 3, the model is validated on linear basis.

5.2. Nonlinear analysis

For nonlinear analysis, the load is increased from 1.0 to 15.0 kPa with increments of 0.5 kPa. The center-of-pane deflection of both panes is recorded for each load and for both boundary conditions. The results are presented in Fig. 13. The experimental results from [16] fit between the two analysis results, but closer to BC_{free} as expected. The relative error between BC_{free} and experimental results varies between 7.4 % and 18.0 %. The error is the largest for small loads and deflections, e.g., 18.0 % corresponds to an absolute error of 0.16 mm for pane 2 in IGU B. The measuring instruments may be one source for errors; they are generally more accurate for higher loads. Further, the supporting structure in the experiments may restrain the in-plane translation and rotation of the edges to some degree, which results in stiffer bending. Since the general trend is correct and the results are conservative (BC_{free}), the model is validated and may be used in further studies.

5.3. Geometric nonlinearity and boundary conditions on the cavity pressure variation

The cavity pressure variation is plotted for loads from 1.0 to 15.0 kPa with increments of 0.5 kPa for three cases: (1) ANSYS nonlinear with BC_{free}; (2) ANSYS nonlinear with BC_{ss}; (3) linear (BAM). Results for IGU A are presented in Fig. 14. Clearly, the geometric nonlinearities have an effect on the cavity pressure variation for high pressure levels. More so if the edges have restricted in-plane movement.

5.4. Case study

The individual and combined influence of the load sharing with the geometric nonlinearity on the response of an IGU is studied. The IGU dimensions are: $b = 1500$ mm, $s = 20$ mm, $t_1 = t_2 = 10$ mm and $a/b = 1,2$. The dimensions are chosen to have a reasonable large window where both effects are significant. The constituent material properties used are presented in Table 4. The influence of the gravity on the results has been verified to be small,[5] and hence, it is neglected. The mesh size

[5] Adding gravity in the same direction as $\bar{p}$ increases the required minimum thickness roughly 0.1 to 0.2 mm of those presented in Table 5 for NL.LS case.

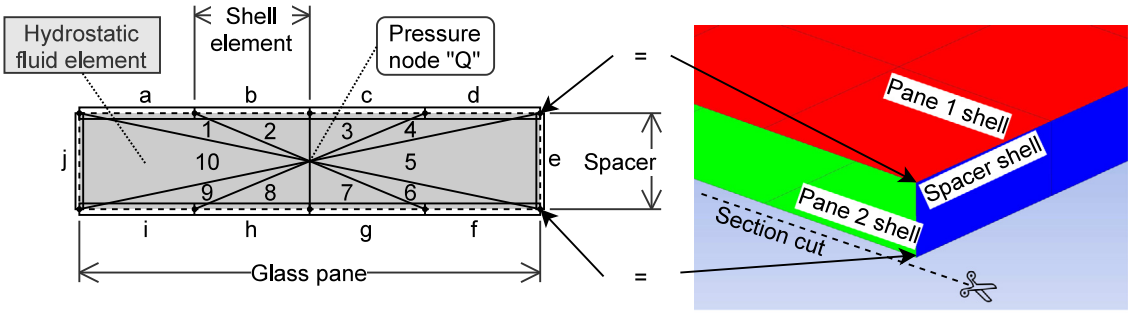

Fig. 9. Illustration of IGU model cross-section on the left-hand side. Letters and numbers represents the structural shell elements and hydrostatic fluid elements, respectively. The dashed line is the mid-plane of the shell elements. Gray colored area is gas. A section cut of the meshed model in ANSYS on the right-hand side (HSFLD242 element not visible).

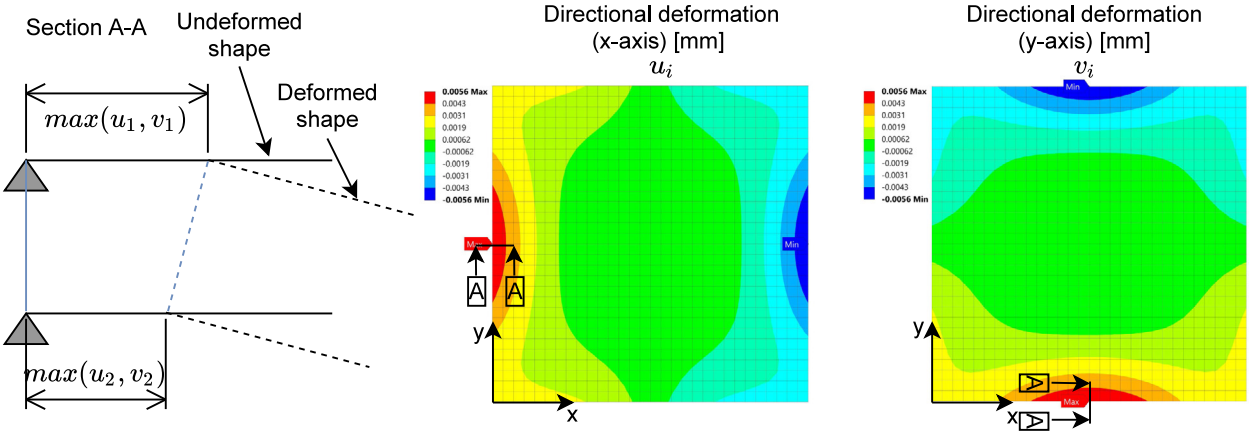

Fig. 10. In-plane movement of the edges. In square IGU, the edges experience equal contraction; $max(u_1) = max(v_1)$ and $max(u_2) = max(v_2)$. In rectangular IGU, the longer side (a) experiences larger contraction than the shorter side (b); $max(u_1) < max(v_1)$ and $max(u_2) < max(v_2)$.

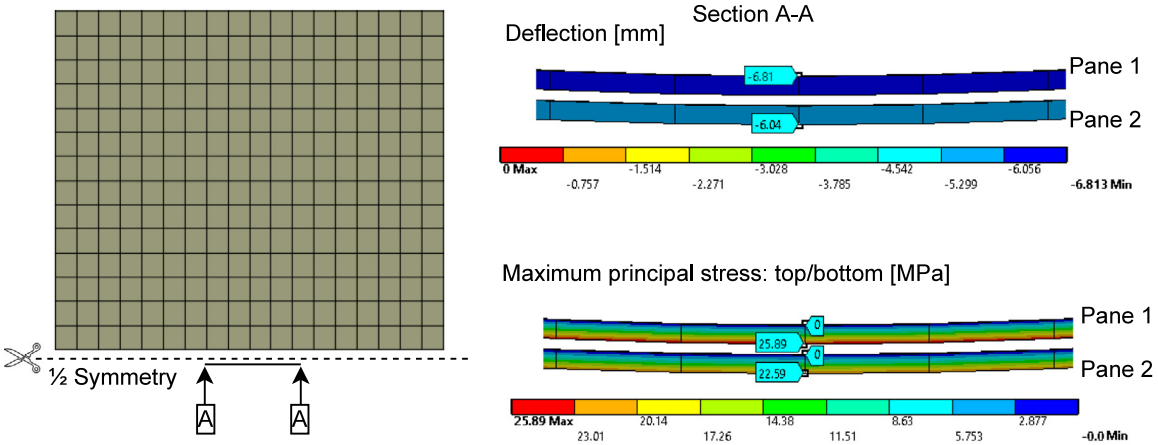

Fig. 11. Deflection and maximum principal stress of both panes under uniformly distributed load acting on pane 1. Directly loaded pane always deflects more due to the compressibility of the gas (6.81 > 6.04). Maximum principal stress is 0 on compression side of both panes. Maximum is at tension side of the directly loaded pane. Thick-shell visuals are activated for these shell elements for distinguishing between top and bottom stress.

in the model is 50 × 50 mm^2 and 50 × 20 mm^2 for glass and for spacers, respectively.

Uniformly distributed load is varied from 1.0 kPa to 30.0 kPa. Only BC_{free} boundary condition is used in nonlinear analysis. Center-of-pane deflection and maximum principal stress of the directly loaded pane (pane 1) is recorded for each load. The results are presented in Fig. 15.

The benefit of considering the load sharing and the geometric nonlinearity is clearly visible. The IGU can withstand more load when the effects are included, compared to linear approach suggested by the classification societies. The maximum principal stress shifts from the middle of the pane to the corner in high pressure levels in nonlinear analysis (Fig. 16). This is due to the initially right-angled corner taking an acute angle after deformation, which induces large shear stresses.

Table 4
Properties of the constituent materials.

	Glass	Spacer	Gas
E [MPa]	70000	0.01	0
ν [–]	0.23	0.01	0
ρ [kg/m^3]	0[a]	0[a]	1.7e−18

[a]Self weight not considered in the analyses.

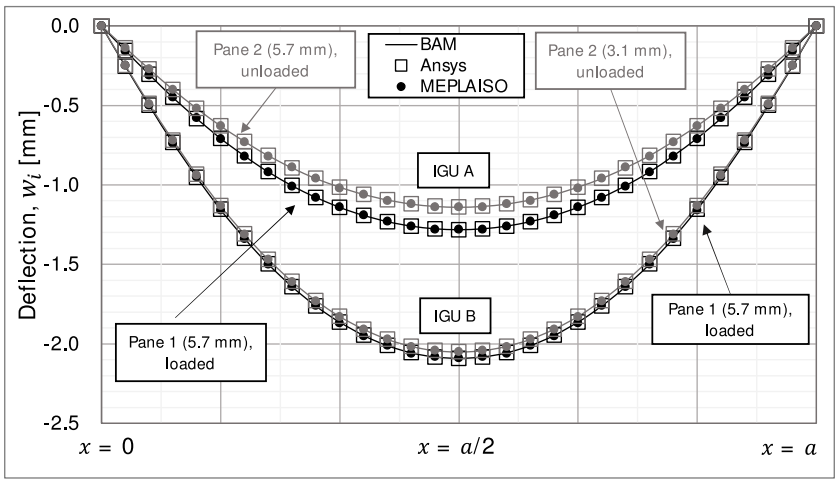

Fig. 12. Deflection of both panes of both IGUs (A and B) every 42 mm from $x = 0$ to $x = a$ along line $b/2$ (middle).

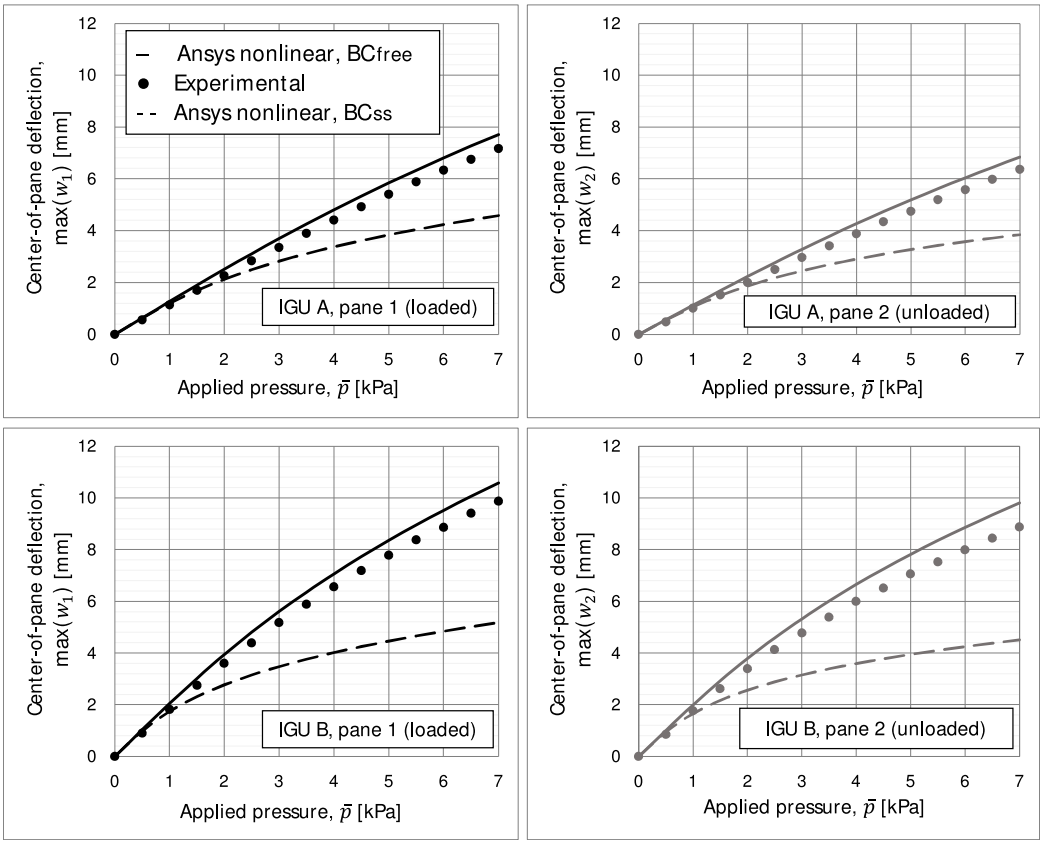

Fig. 13. Comparison of center-of-pane deflection between ANSYS nonlinear results and experimental results from [16]. Boundary conditions are defined in Fig. 6.

This can also be observed in Fig. 15 where the lines have discontinuities (red lines).

In those cases however, the shift occurs past the 40 MPa stress criterion due to the relatively low compliance of the panes (large "t_1"&"t_2" and small "b"). Higher the compliance, earlier the shift. If IGUs are designed to meet the stress criterion using the presented method and boundary condition, the resulting thicknesses are thin enough to have the maximum principle stress at the corner. This can be observed in Fig. 17 where the thickness to width ratios are plotted for multiple aspect ratios, like earlier in Fig. 2. When the dashed line (linear with load sharing) and the solid line (nonlinear with load sharing) are separated, the maximum principle stress is at the corner. When they merge, it shifts back to the middle of the pane. Similarly for the dotted line (nonlinear without load sharing) and the circular marks (standard approach). The benefit of the geometric nonlinearity on the thickness determination varies.

Looking at the bottom row of Fig. 17, the maximum difference to standard results in nonlinear analyses peaks at some aspect ratio, depending on the applied load. Without load sharing, it is the highest around aspect ratios of 2.2, 1.2 and 1.0 for loads 2.5 kPa, 7.5 kPa and 15.0 kPa, respectively. With load sharing, the corresponding aspect ratios are 1.8, 1.8 and 1.2. Considering only the load sharing (linear), the difference is nearly constant for all aspect ratios. Overall, the difference varies between 0 % and 54 %.

As an example, using a square IGU with a side length of 1500 mm, the required minimum thickness can be calculated by extracting the

Table 5
Required minimum pane thicknesses for a square IGU ($b = 1500$ mm, $s = 20$ mm, $t_r = t_1 = t_2$) by different design methods column-wise for three different load cases. Maximum in-plane movement ($\max(u_1, v_1)$ and $\max(u_2, v_2)$) of the edges as presented in Fig. 10. Abbreviations: "STD&CS" is Standard and Classification Societies; "L.LS" is linear with load sharing; "NL" is nonlinear without load sharing; "NL.LS" is nonlinear with load sharing.

$\bar{p}$ [kPa]	2.5				7.5				15.0			
Method	STD&CS	L.LS	NL	NL.LS	STD&CS	L.LS	NL	NL.LS	STD&CS	L.LS	NL	NL.LS
(t_r/b)E-03 [–]	4.20	2.92	3.00	2.10	7.27	5.12	5.48	3.84	10.28	7.45	9.72	5.81
t_r [mm]	6.3	4.4	4.5	3.2	10.9	7.7	8.2	5.8	15.4	11.2	14.6	8.7
$\max(u_1, v_1)$ [mm]	–	–	0.47	0.49	–	–	0.37	0.43	–	–	0.13	0.35
$\max(u_2, v_2)$ [mm]	–	–	–	0.47	–	–	–	0.38	–	–	–	0.27

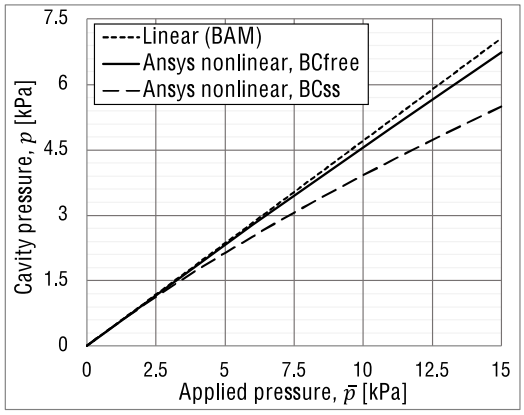

Fig. 14. IGU A generated cavity pressure for loads from 1.0 kPa to 15.0 kPa.

t_r/b values from Fig. 17 for all the design methods and load cases. The results in Table 5 show how much thinner the glass panes in insulating glass units can be designed. The thickness can be reduced by 3.1 mm, 5.8 mm, and 6.7 mm for loads of 2.5 kPa, 7.5 kPa and 15.0 kPa, respectively, when both effects are considered. These correspond to weight reduction of 49.2 %, 46.8 % and 43.5 %, respectively, in glass. Furthermore, the maximum in-plane movement of the edge is 0.49 mm for the thinnest glass pane. Typically an overlap of at least 10 mm is required between the glass pane and the support. Hence, the observed movement does not lead the pane to slip out of the support under design loads, assuming that there is no excessive deformation of the support structure.

6. Discussion

Majority of the ship windows are insulating glass units (IGUs) consisting of two glass panes and a hermetically sealed cavity. Their combined area can reach to up to thousands of square meters in modern cruise ships. Furthermore, a large concentration of IGUs can often be found on the top structures of the ships. For instance, the SkyDome in M/S Iona is located on the sun deck with a glazed area of 970 m^2 (Fig. 1). Hence, the design of ship's glass panes is critical not only for the weight of the ship, but also for the stability. The classification rules (e.g. [11,12]) assume that the cavity pressure does not exist and linear plate theory is valid, which may lead to thicker glass pane designs than necessary.

Analytical methods, BAM [19] and MEPLA ISO [22], can be used to determine the glass pane thickness in IGUs on linear basis, including the load sharing effect. This already allows for considerable thickness reduction compared to the classification rule design approach (Table 5). The load sharing occurs as long as the cavity remains sealed and the panes are compliant, i.e. thin and large. While the analytical methods are fast to use, they are limited to certain glass shapes and boundary conditions, and they neglect the geometric nonlinearity.

Finite Element Method can be used to include the geometric nonlinearity. Its positive influence on the generated cavity pressure is presented in Fig. 14, and on the deflections and stresses of the panes in Fig. 15. The stress reduction potentially allows for even further reduction of the thicknesses (Table 5). However, the benefit of the geometric nonlinearity in addition to the load sharing is a function of the aspect ratio of the panes and the magnitude of the applied load, as presented in Fig. 17. The linear and nonlinear results are equivalent at larger aspect ratios. Most of the largest windows are, however, located on top decks, i.e. design pressure is at the lower end, and they have reasonable low aspect ratios. And with these two conditions, the considered effects are the most beneficial, assuming that the allowable stress is 40 MPa and the boundary conditions allow for in-plane sliding of the panes (Fig. 6).

This boundary conditions was used in the case study because good agreement was found between the presented FE model and the experimental results by McMahon et al. [16]. The simply supported condition that did not allow for in-plane sliding appeared to underestimate the deflections heavily. Achieving either condition in real life is very difficult, if not impossible, with glass panes. Similarly, defining a real life condition exactly at some point between the limits is difficult. Hence, using unrestricted sliding condition is a better conservative approach.

Allowing the panes to slide shifted the position of the maximum principal stress from middle of the panes to the corners, like reported in [17]. This indicates that when the panes are inspected for surface cracks/flaws, then the corners should also be of interest. The thinner the panes are and the larger the short side is, the smaller the required load is to shift the position of the maximum stress to the corner. On the other hand, increasing the aspect ratio increases the required load for the shift to occur.

Considering the results of this study and the fact that the IGUs have become a weight critical component in cruise ships, Finite Element Method is preferred over the alternative methods [17,18,22] for determining the thickness of the glass panes.

7. Conclusion

This paper studied the effect of the load sharing and geometric nonlinearity on the thickness determination of rectangular glass panes in insulating glass units used in cruise ships. For this purpose, a Finite Element Method was used. The gas in the cavity was modeled with hydrostatic fluid element (HSFLD242) and the glass panes with structural shell elements (SHELL181). Their interaction is embedded in the model and it follows the ideal gas law. The FE model was in good agreement with analytical methods and experimental results from scientific literature on linear and nonlinear basis, respectively.

From the study results it can be concluded that the current glass pane thickness determination rules by different societies for ship classification results in thicker constructions than necessary. This is because: (1) the equations for the glass pane thickness determination are based on linear-elastic, small deformation, plate theory; (2) the load sharing effect in insulating glass units is not considered.

Taking in account the interaction of the panes and the geometric nonlinearity, the stress in the glass panes reduces significantly. Because the classification rules prescribe allowable maximum principal stress, reduced stress allows for reduced thickness. The case study on typical ship windows showed that the thickness could potentially be reduced

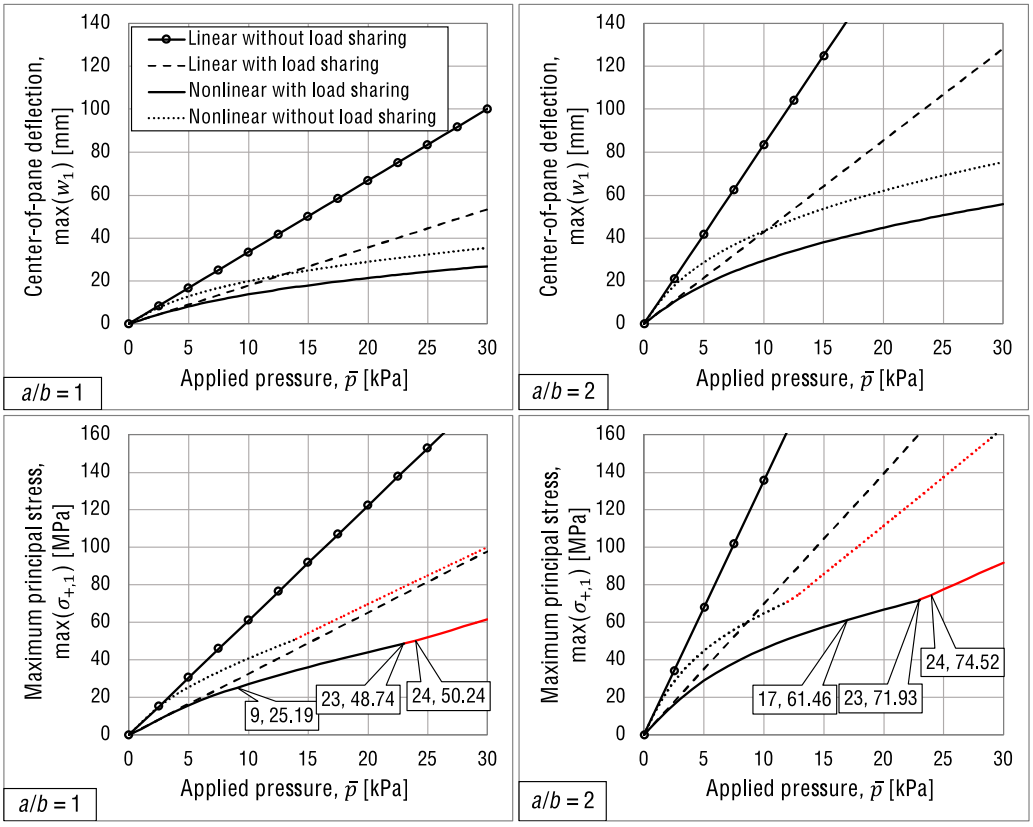

Fig. 15. Pane 1 center-of-pane deflection and maximum principal stress of IGU (b = 1500 mm, s = 20 mm, $t_1 = t_2$ = 10 mm) for two aspects ratios (1 & 2) subjected to uniformly distributed load from 1.0 kPa to 30.0 kPa. Results without load sharing corresponds to a case with only one glass pane (no gas).

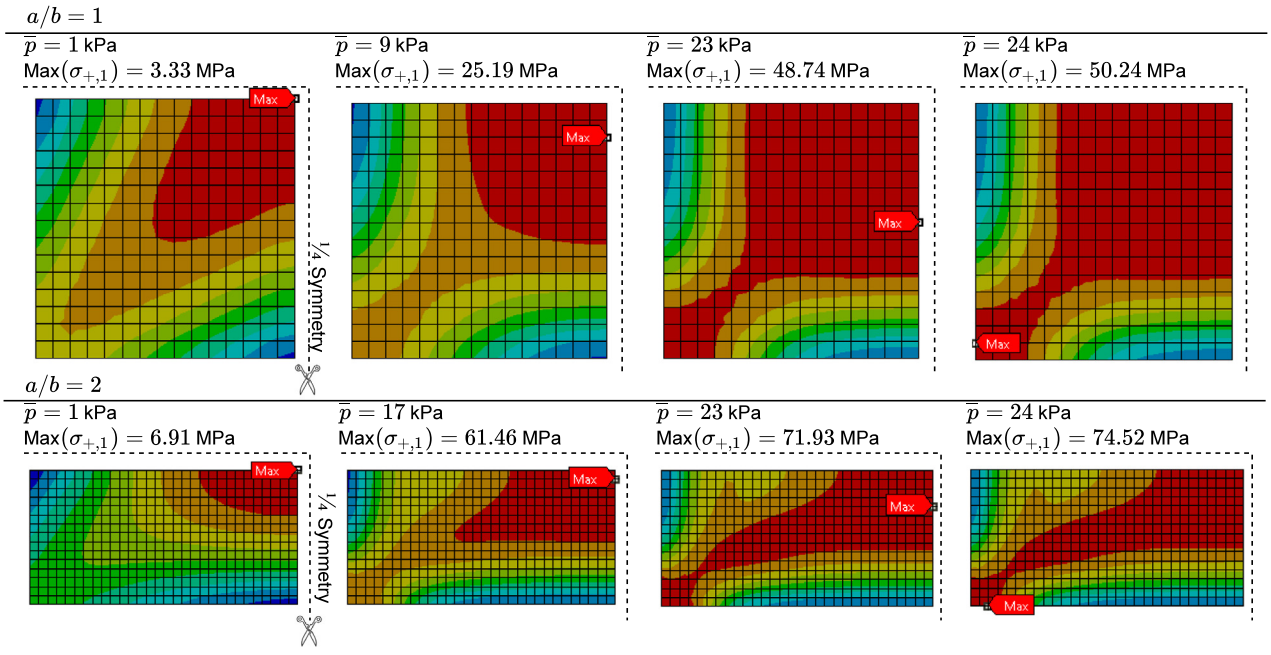

Fig. 16. Maximum principal stress shift from middle of the pane to the corner for aspect ratios of 1 and 2 in the top and bottom row, respectively. The analyses corresponds to results in Fig. 15 (nonlinear with load sharing).

between 26–54 %, 26–35 % and 0–35 % by considering both of the effects, only the load sharing and only the geometric nonlinearity, respectively.

The case study was performed for an rectangular IGU with certain dimensions and assumptions. For future work, the interest is in finding an optimum IGU design. For this, an optimization tool using ANSYS and MATLAB could be built under defined design space for rectangular, triangular and circular IGUs. For fully defining the design space, it is suggested to perform more experimental work on insulating glass units to study the influence of the boundary conditions, laminated glasses,

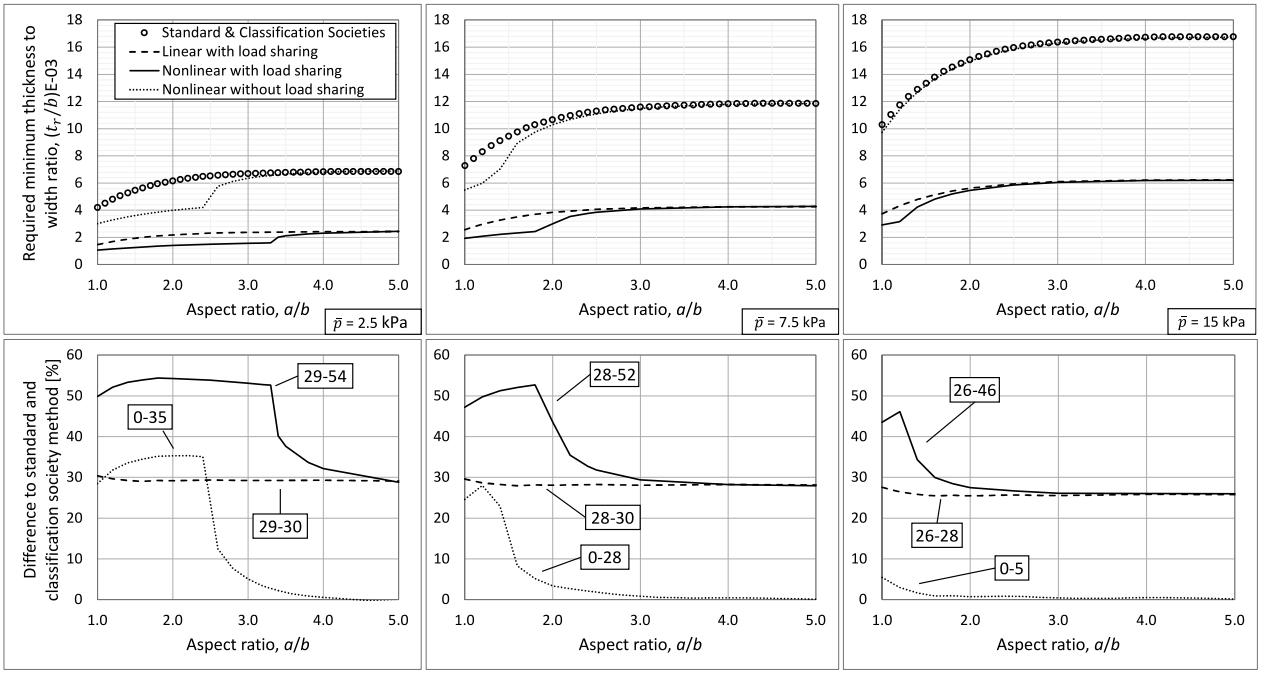

Fig. 17. On top row is required minimum thickness to width ratio for multiple aspect ratios, a comparison between different design methods. On bottom row is the corresponding percentual difference to the standard and classification society method.

and the edge seal system on the response. Furthermore, as the strength of glass has a relatively large variation, a study should be conducted to determine if using safety factor of 4 for the strength is feasible with large glass panes.

CRediT authorship contribution statement

Janne Heiskari: Conceptualization, Formal analysis, Investigation, Methodology, Validation, Writing – original draft. **Jani Romanoff:** Conceptualization, Funding acquisition, Resources, Supervision, Writing – review & editing. **Aleksi Laakso:** Conceptualization, Resources, Writing – review & editing. **Jonas W. Ringsberg:** Supervision, Writing – review & editing.

Declaration of competing interest

The authors declare that they have no known competing financial interests or personal relationships that could have appeared to influence the work reported in this paper.

Acknowledgments

This study was funded by Meyer Turku Oy, Finland and Aalto University, Finland. A special acknowledgment to Ari Niemelä, head of hull basic design at Meyer Turku Oy, for his helpful comments and discussion in developing this research.

Appendix. Determination of monolithic thickness

The thickness for single rectangular glass pane is determined according to the equations in Table 1. The variables are design load (H, q), length of shorter side (b), factor related to aspect ratio (β) and allowable design flexural stress of glass (σ_a). The design flexural stress is 40 MPa for thermally toughened and chemically strengthened glass. It is obtained from characteristic failure strength of glass (160 MPa) using safety factor of 4, as suggested by ISO 11336-1 [14]. Required design pressures vary from 2.5 to 50.0 kPa depending on the location of the window and applied rule or standard. Typically, 2.5 kPa is used for windows located on the upper superstructure deck sides or the aft. In this study, 2.5 kPa, 7.5 kPa and 15.0 kPa are used to cover reasonable loading conditions for the studied windows. Because the windowpanes are brittle material, the maximum principal stress is used as a stress criterion. The maximum principal stress is:

$$\sigma_+ = \frac{\sigma_x + \sigma_y}{2} + \sqrt{\left(\frac{\sigma_x - \sigma_y}{2}\right)^2 + \sigma_{xy}^2}. \tag{A.1}$$

Where the normal stresses, σ_x and σ_y, are:

$$\begin{aligned} \sigma_x &= \frac{6M_x}{t^2} \\ \sigma_y &= \frac{6M_y}{t^2}. \end{aligned} \tag{A.2}$$

The bending moments, M_x and M_y, for rectangular Kirchhoff–Love plates subjected to uniformly-distributed load, $\bar{p}$, are:

$$\begin{aligned} M_x &= \frac{16\bar{p}}{\pi^4}\sum_{m=1}^{\infty}\sum_{n=1}^{\infty}\frac{\frac{m^2}{a^2}+\nu\frac{n^2}{b^2}}{mn\left(\frac{m^2}{a^2}+\frac{n^2}{b^2}\right)^2}\sin\left(\frac{m\pi x}{a}\right)\sin\left(\frac{n\pi y}{b}\right) \\ M_y &= \frac{16\bar{p}}{\pi^4}\sum_{m=1}^{\infty}\sum_{n=1}^{\infty}\frac{\frac{n^2}{b^2}+\nu\frac{m^2}{a^2}}{mn\left(\frac{m^2}{a^2}+\frac{n^2}{b^2}\right)^2}\sin\left(\frac{m\pi x}{a}\right)\sin\left(\frac{n\pi y}{b}\right). \end{aligned} \tag{A.3}$$

Additionally, the deflection of rectangular Kirchhoff's plate subjected to uniformly distributed load is:

$$w(x,y) = \frac{16\bar{p}}{\pi^6 D}\sum_{m=1}^{\infty}\sum_{n=1}^{\infty}\frac{1}{mn\left(\frac{m^2}{a^2}+\frac{n^2}{b^2}\right)^2}\sin\left(\frac{m\pi x}{a}\right)\sin\left(\frac{n\pi y}{b}\right). \tag{A.4}$$

References

[1] H.W. Leheta, A.S. Elhanafi, S.F. Badran, A numerical study of the ultimate strength of Y-deck panels under longitudinal in-plane compression, Thin-Walled Struct. 100 (2016) 134–146, http://dx.doi.org/10.1016/j.tws.2015.12.013, URL https://www.sciencedirect.com/science/article/pii/S0263823115301762.

[2] H. Wang, Y. Cheng, J. Liu, P. Zhang, Hydroelastic behaviours of laser-welded lightweight corrugated sandwich panels subjected to water impact: Experiments and simulations, Thin-Walled Struct. 146 (2020) 106452, http://dx.doi.org/10.1016/j.tws.2019.106452, URL https://www.sciencedirect.com/science/article/pii/S0263823119301259.
[3] J. Jelovica, J. Romanoff, R. Klein, Eigenfrequency analyses of laser-welded web–core sandwich panels, Thin-Walled Struct. 101 (2016) 120–128, http://dx.doi.org/10.1016/j.tws.2016.01.002, URL https://www.sciencedirect.com/science/article/pii/S0263823116300027.
[4] W. He, J. Liu, S. Wang, D. Xie, Low-velocity impact behavior of X-Frame core sandwich structures – experimental and numerical investigation, Thin-Walled Struct. 131 (2018) 718–735, http://dx.doi.org/10.1016/j.tws.2018.07.042, URL https://www.sciencedirect.com/science/article/pii/S0263823118301307.
[5] V.T. Doan, B. Liu, Y. Garbatov, W. Wu, C. Guedes Soares, Strength assessment of aluminium and steel stiffened panels with openings on longitudinal girders, Ocean Eng. 200 (2020) 107047, http://dx.doi.org/10.1016/j.oceaneng.2020.107047, URL http://www.sciencedirect.com/science/article/pii/S0029801820301219.
[6] V. Crupi, G. Epasto, E. Guglielmino, Comparison of aluminium sandwiches for lightweight ship structures: Honeycomb vs. foam, Mar. Struct. 30 (2013) 74–96, http://dx.doi.org/10.1016/j.marstruc.2012.11.002, URL http://www.sciencedirect.com/science/article/pii/S0951833912000810.
[7] J. Gordo, C.G. Soares, Tests on ultimate strength of hull box girders made of high tensile steel, Mar. Struct. 22 (4) (2009) 770–790, http://dx.doi.org/10.1016/j.marstruc.2009.07.002, URL http://www.sciencedirect.com/science/article/pii/S0951833909000495.
[8] I. Lillemäe, H. Remes, J. Romanoff, Influence of initial distortion of 3 mm thin superstructure decks on hull girder response for fatigue assessment, Mar. Struct. 37 (2014) 203–218, http://dx.doi.org/10.1016/j.marstruc.2014.04.001, URL http://www.sciencedirect.com/science/article/pii/S095183391400029X.
[9] B. Barsotti, M. Gaiotti, C.M. Rizzo, Recent industrial developments of marine composites limit states and design approaches on strength, J. Mar. Sci. Appl. (2020) 1–14, http://dx.doi.org/10.1007/s11804-020-00171-1.
[10] Iona SkyDome | Francis Design, URL https://www.francisdesign.com/project/iona-skydome/.
[11] Lloyd's register, rules and regulations for the classification of ships, July, 2020.
[12] DNV GL, Rules for Classification: Ships, Part 3 Hull, 2020, Chapter 12 Openings and closing appliances, Edition July.
[13] RINA, Rules for the Classification of Ships, Pt B, Ch 9, Sec 9, 2019, Arrangement of hull and superstructure openings.
[14] ISO 11336-1:2012, Large yachts - Strength, weathertightness and watertightness of glazed openings - Part 1: Design criteria, materials, framing and testing of independent glazed openings, International Organization for Standardization, Geneva.
[15] B. Gerlach, W. Fricke, Experimental and numerical investigation of the behavior of ship windows subjected to quasi-static pressure loads, Mar. Struct. 46 (2016) 255–272, http://dx.doi.org/10.1016/j.marstruc.2016.02.001, URL http://www.sciencedirect.com/science/article/pii/S095183391600006X.
[16] S. McMahon, H. Scott Norville, S.M. Morse, Experimental investigation of load sharing in insulating glass units, J. Archit. Eng. 24 (1) (2018) 04017038.
[17] C.G. Vallabhan, G.D. Chou, Interactive nonlinear analysis of insulating glass units, J. Struct. Eng. 112 (6) (1986) 1313–1326.
[18] J.-D. Wörner, X. Shen, B. Sagmeister, Determination of load sharing in insulating glass units, J. Eng. Mech. 119 (2) (1993) 386–392.
[19] L. Galuppi, G. Royer-Carfagni, Betti's analytical method for the load sharing in double glazed units, Compos. Struct. 235 (2020) 111765, http://dx.doi.org/10.1016/j.compstruct.2019.111765, URL http://www.sciencedirect.com/science/article/pii/S0263822319325541.
[20] L. Galuppi, G. Royer-Carfagni, Green's functions for the load sharing in multiple insulating glazing units, Int. J. Solids Struct. 206 (2020) 412–425, http://dx.doi.org/10.1016/j.ijsolstr.2020.09.030, URL http://www.sciencedirect.com/science/article/pii/S0020768320303802.
[21] SFS-EN 16612:2019, Glass in Building. Determination of the Lateral Load Resistance of Glass Panes by Calculation, Finnish Standards Association SFS.
[22] D. Bohmann, Mepla ISO freeware - software for structural glass design, 2020.
[23] M. Haldimann, A. Luible, M. Overend, Structural Use of Glass, IABSE, Zurich, Switzerland, 2008, http://dx.doi.org/10.2749/sed010.
[24] E. Ventsel, T. Krauthammer, Thin Plates and Shells: Theory: Analysis, and Applications, CRC Press, 2001.
[25] S. Buddenberg, P. Hof, M. Oechsner, Climate loads in insulating glass units: comparison of theory and experimental results, Glass Struct. Eng. 1 (1) (2016) 301–313, http://dx.doi.org/10.1007/s40940-016-0028-z.
[26] Ansys Mechanical APDL 2020 R1. Theory Reference. Chapter 14: Analysis tools - 14.11. Newton–Raphson Procedure.
[27] Ansys Mechanical APDL 2020 R1. Theory Reference. Chapter 13: Element Library - 13.242. HSFLD242-3-D Hydrostatic Fluid.
[28] L. Galuppi, Practical expressions for the design of DGUs. The BAM approach, Eng. Struct. 221 (2020) 110993, http://dx.doi.org/10.1016/j.engstruct.2020.110993, URL http://www.sciencedirect.com/science/article/pii/S0141029619351879.
[29] A. Vuolio, Structural behaviour of glass structures in facades, (Licentiate thesis), Helsinki University of Technology, 2003.
[30] RF-GLASS: Structural Analysis and Design of Glass Panes | Dlubal Software.
[31] C. Bedon, C. Amadio, Mechanical analysis and characterization of IGUs with different silicone sealed spacer connections - part 2: modelling, Glass Struct. Eng. 5 (3) (2020) 327–346, http://dx.doi.org/10.1007/s40940-020-00123-9.
[32] C. Bedon, C. Amadio, A linear formulation for the ULS design of glass elements under combined loads: application to IGUs, Glass Struct. Eng. 3 (2) (2018) 289–301, http://dx.doi.org/10.1007/s40940-018-0060-2.
[33] J. Heiskari, On the Design Criteria of Large Insulating Glass Structures in Cruise Ships, (Master's thesis), Aalto University and Chalmers University of Technology, 2020.
[34] M. Teotia, R. Soni, Applications of finite element modelling in failure analysis of laminated glass composites: A review, Eng. Fail. Anal. 94 (2018) 412–437, http://dx.doi.org/10.1016/j.engfailanal.2018.08.016, URL http://www.sciencedirect.com/science/article/pii/S135063071830493X.
[35] Ansys Mechanical APDL 2020 R1. Element Reference. Chapter 7: Element Library - 4-Node Structural Shell.
[36] Ansys Mechanical APDL 2020 R1. Element Reference. Chapter 7: Element Library - 3-D Hydrostatic Fluid.